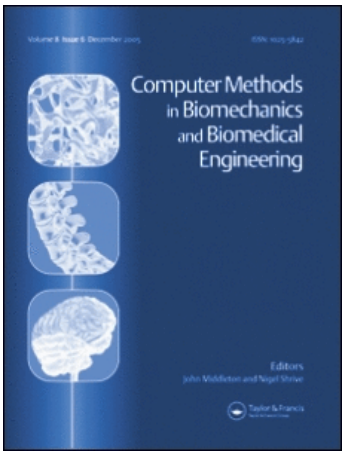

Computer Methods in Biomechanics and Biomedical Engineering
Publication details, including instructions for authors and subscription information:
http://www.informaworld.com/smpp/title~content=t713455284

Improving the damage accumulation in a biomechanical bone remodelling model

J. M. Restrepo [a]; R. Choksi [b]; J. M. Hyman [c]; Y. Jiang [c]
[a] Department of Mathematics and Department of Physics, University of Arizona, Tucson, AZ, USA [b] Department of Mathematics, Simon Fraser University, Burnaby, BC, Canada [c] Theoretical Division, Los Alamos National Laboratory, Los Alamos, NM, USA

First Published:June2009

To cite this Article Restrepo, J. M., Choksi, R., Hyman, J. M. and Jiang, Y.(2009)'Improving the damage accumulation in a biomechanical bone remodelling model',Computer Methods in Biomechanics and Biomedical Engineering,12:3,341 — 352
To link to this Article: DOI: 10.1080/10255840802609404
URL: http://dx.doi.org/10.1080/10255840802609404

Computer Methods in Biomechanics and Biomedical Engineering
Vol. 12, No. 3, June 2009, 341–352

Taylor & Francis
Taylor & Francis Group

Improving the damage accumulation in a biomechanical bone remodelling model

J.M. Restrepo[a], R. Choksi[b], J.M. Hyman[c] and Y. Jiang[c]*

[a]*Department of Mathematics and Department of Physics, University of Arizona, Tucson, AZ, USA;* [b]*Department of Mathematics, Simon Fraser University, Burnaby, BC, Canada;* [c]*Theoretical Division, Los Alamos National Laboratory, Los Alamos, NM, USA*

(*Received 19 May 2008; final version received 30 September 2008*)

We extend, reformulate and analyse a phenomenological model for bone remodelling. The original macrobiomechanical model (MBM), proposed by Hazelwood et al. [J Biomech 2001; 34:299–308], couples a population equation for the cellular activities of the basic multicellular units (BMUs) in the bone and a rate equation to account for microdamage and repair. We propose to account for bone failure under severe overstressing by incorporating a Paris-like power-law damage accumulation term. The extended model agrees with the Hazelwood et al. predictions when the bone is under-stressed, and allows for suitably loaded bones to fail, in agreement with other MBM and experimental data regarding damage by fatigue. We numerically solve the extended model using a convergent algorithm and show that for unchanging loads, the stationary solution captures fully the model behaviour. We compute and analyse the stationary solutions. Our analysis helps guide additional extensions to this and other BMU activity based models.

Keywords: bone; remodelling; damage accumulation; BMU; biomechanics; numerical

1. Introduction

Bone is a dynamic tissue that adapts its internal microstructure to its physiological and mechanical environment through a process known as bone remodelling. Live bone is continuously renewed and microdamage, accumulated by fatigue or creep, is continuously repaired. It is commonly accepted that bone remodelling is carried out by basic multicellular units (BMUs) consisting of bone resorbing osteoclasts and bone forming osteoblasts working in concert.

When the BMUs are activated, there is an initial period of time, called the resorption period, where osteoclasts break down bone through resorption of bone tissue. This is followed, after a brief period of inactivity, by the reversal period where new bone tissue is formed. Until recently, most bone remodelling models were based on phenomenological descriptions of these activities as measured by the average change of bone porosity or density through the coordinated activities of osteoclasts and osteoblasts.

Recent advanced biologically based bone remodelling models (Hernandez et al. 2000, 2001; Hazelwood et al. 2001; Doblaré et al. 2004; García-Aznar et al. 2005) couple these BMU bone cell activities with the mechanical damage fatigue dynamics related to the accumulation and removal of bone tissue. These coupled models, which we will refer to as macrobiomechanical models (MBM), have yielded new insights by relating the cell activities during bone remodelling to the mechanical stimulus of the bone. The MBM proposed by Hazelwood, Martin, Rashid and Rodrigo (2001) (referred to as HMRR) was the first model coupling the BMU dynamics and microdamage. It has been used to study the long-term effects of biphosphonate on the development of trabecular bone (Nyman et al. 2004a), and been used in combination with a finite element code to assess different types of knee replacement strategies (Nyman et al. 2004b).

In Section 2, we start by reformulating the HMRR to clarify the simple and robust structure of the population model for the BMUs and the rate equation to account for microdamage. The reformulated model simplifies the analysis, allowing us to mathematically characterise the behaviour of the model (Section 3). The reformulation also balances the space and time scales, which can greatly reduce the numerical errors when simulating the equations. We obtain explicit solutions for the asymptotic (long-time) solutions of the model. These steady states provide a global perspective of the model outcomes and constrain the equilibrium values of bone porosity p and microdamage D.

The original HMRR model uses a constant rate of accumulation of damage, which results in an upper bound for bone damage. Experimental data (Caler and Carter 1989; Pattin et al. 1996; Cotton et al. 2003), show that repeated large loading continually weakens bone, and if the load is large enough the bone will eventually fail, i.e. damage becomes catastrophic.

The reformulated HMRR model sheds light on how to extend the model and account for bone failure under severe over-stress. Equally important, it suggests a damage repair mechanism that depends on BMU activity. We modify the model by replacing the damage accumulation

*Corresponding author. Email: jiang@lanl.gov

ISSN 1025-5842 print/ISSN 1476-8259 online

DOI: 10.1080/10255840802609404
http://www.informaworld.com

term by a Paris-like law for fracture mechanics (cf. Suresh 1991). In Section 4, we verify that the modified model solutions agree with the original HMRR model when the bone is under-stressed, and show how it accounts for failure when the bone is over-stressed and the damage repair cannot counteract the growth term. Thus, the new model extends the range of validity for the HMRR model to wider range of mechanical dynamics.

The reformulated model has other desirable qualities, not the least of which is that it is now amenable to mathematical and numerical analysis. The extreme disparity in size of variables and parameters in the model can easily lead to numerical loss-of-precision errors, and the solutions for larger errors can qualitatively differ from the converged solution. The well-balanced formulation of the extreme range of parameters and spatio-temporal scales reduces the impact of computer round-off errors when numerically solving the equations. We solved the integro-differential equations using a convergent variable order stiff solver of type 'backward difference formula' (see Iserles 1996) inside an adaptive trapezoidal quadrature for the integrals. We confirmed the numerical solution had a second order convergence rate as the time step, Δt, was decreased. This is in agreement with the theoretical convergence estimate of the method.

These numerical experiments verify the need to be especially careful when formulating and solving models with a vast range of space and time scales. The mathematical analysis is shown to be instrumental in providing a guide to the accurate numerical solution of the equations. It is also instrumental in permitting us to show how close the HMRR model is to other MBM models.

Section 6 summarises our results and the ways in which the model can be simplified, without sacrificing accuracy, and concludes the paper by suggesting paths for improvement of this and other MBM models.

2. The MBM of Hazelwood et al.

MBM models couple the basic biological and mechanical processes for bone remodelling in order to simulate the macromechanical behaviour of bone with simple equations. Their simplicity makes them ideal to test our understanding of macroscopic process. There are a variety of these models and one of our aims is to show that the HMRR model is similar in structure to other MBM's. This unifying exercise is for further developments in the modelling process. We start by recasting the HMRR model so it is more amenable to analysis and less prone to round-off errors in numerical simulations.

2.1 The coupled delay equations

The external mechanical load on a representative volume containing BMUs affects the remodelling activities of the BMUs. This leads to changes in bone porosity, which in turn changes the mechanical response of the bone. The porosity of the bone is a fraction or percentage of the pores within the bone; $p = 0$ corresponds to dense bone, and $p = 1$ corresponds to bone of zero density. The damage is defined as the total crack length per section of area of the bone. Two variables contribute to changes in p and D: a mechanical stimulus Φ, and the BMU activation frequency $f_a(p, D, t)$.

The equations for the porosity p and the damage D are

$$\frac{\mathrm{d}p(t)}{\mathrm{d}t} = A\left(\overline{N_R}(p, D, t) - \overline{N_F}(p, D, t)\right), \tag{1}$$

$$\frac{\mathrm{d}D(t)}{\mathrm{d}t} = K_D\Phi - F_s\, ADf_a(p, D), \tag{2}$$

where $t \geq t_0$ is time, measured in units of days; both $\bar{N}_R$ and $\bar{N}_F$ depend indirectly on the mechanical stimulus. Here K_D is a constant of proportionality (to be discussed further in Section 3), and $F_s = 5\,\mathrm{mm}^{-2}$ is an empirical factor associated with microcrack surface area (see the HMRR paper for details). The initial conditions are given at time t_0 and there are three time intervals associated with the BMU activity, the resorption period T_R, the inactive period T_I and the refilling period T_F. If the modified area A was strictly constant it could easily be scaled out of the equations by redefining time τ, say such that $\mathrm{d}/\mathrm{d}t = A\mathrm{d}/\mathrm{d}\tau$. However,

$$A = \begin{cases} A_0 & \text{if } \Phi \geq \Phi_0; \\ (1/2)A_0(1 + \Phi/\Phi_0) & \text{otherwise,} \end{cases}$$

where A_0 and Φ_0 are constants, the former is associated with the typical area measure, the latter with a threshold on the mechanical stimulus. Equation (1) incorporates the temporal periods for both resorption and refilling via the averages $\overline{N_R} := N_R(t)/T_\mathrm{R}$, and $\overline{N_F} := N_F/T_\mathrm{F}$.

The associated population resorption and refilling densities N_R and N_F at time t are given by

$$\begin{aligned} N_R(t) &= \int_{t-T_\mathrm{R}}^{t} f_a(p(s), D(s))\mathrm{d}s \\ N_F(t) &= \int_{t-(T_\mathrm{R}+T_\mathrm{I}+T_\mathrm{F})}^{t-(T_\mathrm{R}+T_\mathrm{I})} f_a(p(s), D(s))\mathrm{d}s. \end{aligned} \tag{3}$$

These integrals must be defined for small times when their lower limits are negative. (Without loss of generality, we take the initial time $t_0 = 0$ in everything that follows). A simple way to remove any ambiguity from the initial data is to define the prehistory data as an equilibrium solution, but otherwise, initialising the model can be subtle if nothing is known about its behaviour. We will show that the time-dependent behaviour of the model is parametric in the time dependence (if any) of the load: steady state solutions to the full model for steady

loads can be computed for the full range of p and D. To fully define the system of delay equations, for the first full cycle of the BMU unit, i.e. for $t \in [0, T_R + T_I + T_F]$, one must either prescribe initial data for $p(t)$ and $D(t)$; define $\overline{N_R} = N_R/T_R$ and $\overline{N_F} = N_F/T_F$; or define the historical values of the damage component $f_a(s)$ for $s \in [-(T_R + T_I + T_F), 0]$. For $t \leq T_R + T_I + T_F$ the bone model exhibits transient behaviour and, unless the historical data are known, these initial values must be given to fully define the system.

To simplify the notation in Equation (3), define the average population reabsorption density as

$$I(a,b) \equiv \int_a^b f_a(p(s), D(s))\mathrm{d}s.$$

We define the initial conditions for N_R as:

$$N_R(p,D,t) = \begin{cases} I[0,t], & \text{if } t < T_R; \\ I[t - T_R, t], & \text{otherwise}, \end{cases} \tag{4}$$

and set $N_F(p,D,t) = 0$, for $t \leq T_R + T_I + T_F$. The initial time averages are defined as

$$\overline{N_R}(p,D,t) = \begin{cases} I[0,t]/t, & \text{if } t < T_R; \\ I[t - T_R, t]/T_R, & \text{otherwise}, \end{cases} \tag{5}$$

and

$$\overline{N_F}(p,D,t) = \begin{cases} 0 & \text{if } t < T_R + T_I + T_F; \\ I[t - (T_R + T_I + T_F), \\ \quad t - (T_R + T_I)]/T_F & \text{otherwise}. \end{cases} \tag{6}$$

2.2 The physical variables

Given a strain, $\varepsilon = L/E$, the time to fracture is given by the relation $t_f \propto \varepsilon^{-q}$, where $q > 0$ is an empirically adjusted exponent (Caler and Carter 1989; Cotton et al. 2003), E is the elastic modulus of the bone and ε is the strain. The mechanical stimulus is defined as

$$\Phi := \frac{1}{t_f} = R_L \varepsilon^q, \tag{7}$$

where the constant R_L is the loading rate (Martin 1992).

The elastic modulus e of the bone was fit to data in terms of p (see Martin et al. 1998 for details on the fit). HMRR used the following polynomial fit to experimental data,

$$e(p) = 10^5\big(8.83p^6 - 29.9p^5 + 39.9p^4 - 26.4p^3 + 9.08p^2 - 1.68p + 0.237\big). \tag{8}$$

The reader should note that the more conventional material quantities associated with classical mechanics, such as the Poisson ratio, are already subsumed into the empirical fit. (In Hernandez et al. 2000 and 2001, an alternative empirical fit to the Young's modulus is suggested in which the Poisson ratio appears as a defined constant, and hence the same thing could be done here with the empirical prescription of HMRR). The function $e(p)$, shown in Figure 1(a) as a solid line, agrees with the experimental data for low porosity but differs greatly from the data at high porosity values (Martin et al. 1998); of note is that it is non-zero at $p = 1$. We regularised this formula for $p > 0.4$ to obtain

$$E(p) = \begin{cases} e(p) & 0 \leq p \leq 0.4 \\ e(0.4)(1-p)/0.6 & 0.4 < p \leq 1. \end{cases} \tag{9}$$

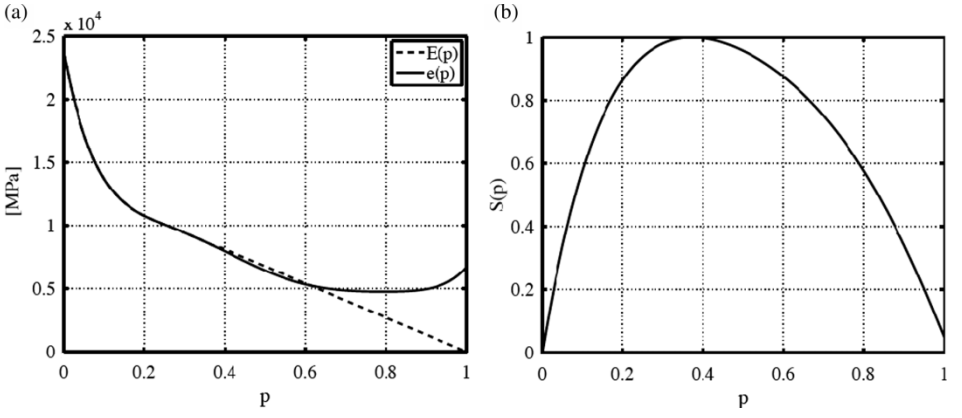

Figure 1. (a) The solid line is the elastic modulus $e(p)$ as defined in HMRR; the dashed line is the regularised version where $E(1) = 0$ defined in Equation (9). (b) The normalised specific surface area $S(p)$, as given by the empirical fit Equation (10).

A superposition of these alternative definitions of the elastic modulus is plotted in Figure 1(a). We discuss further the difference between these two alternatives in Section 5.

The specific surface area, S, is fitted to data, as in Hazelwood et al. (2001) and normalised to the range [0, 1], as

$$S(p) = \frac{\left(28.8p^5 - 101.0p^4 + 134.0p^3 - 93.9p^2 + 32.2p\right)}{S_N}. \tag{10}$$

Here S_N is defined to normalise the maximum of the specific surface area to 1. Figure 1(b) shows the normalised specific surface area.

The BMUs are activated by disuse and microdamages. The BMU activation frequency $f_a(D, p)$ is defined as

$$f_a(p, D) = S(p)(f_{a(\text{disuse})}(p) + f_{a(\text{damage})}(D)). \tag{11}$$

The activity due to disuse is defined as

$$f_{a(\text{disuse})}(p) = \begin{cases} f_{a(\max)}/\left(1 + c_1 \mathrm{e}^{c_2\Phi(p)}\right) & \text{if } \Phi < \Phi_0; \\ 0 & \text{otherwise,} \end{cases} \tag{12}$$

where c_1 and c_2 are constants, Φ_0 is an empirically derived threshold mechanical stimulus estimated from cyclic strain levels needed to maintain cortical bone mass at equilibrium.

The porosity of Haversian canals is less than 10% for average people below 50 years of age, and at worst around 30% for females over 80 years old (Wang and Ni 2003). The parameters (Φ_0 and f_{a0}) in HMRR were derived for Haversian canals or cortical bones for the limited range of porosity (e.g. $p < 0.3$) where their model is valid.

The damage component of the activation frequency is defined by

$$f_{a(\text{damage})}(D) = \frac{f_{a(\max)}}{1 + c_3 \mathrm{e}^{c_4 D}},$$

where c_3 and c_4 are constants ($c_4 < 0$), the values of which may be inferred from Table 1.

Since the modification to elastic modulus used in HMRR by our regularised version is only significantly different for $p > 0.4$, the function $f_{a(\text{disuse})}$ does not change and thus the activation frequency remains the same. Therefore, the p evolution equation does not change either. The main effect of this regularisation is in the first term, $K_D\Phi$, in the damage equation (2) wherein the mechanical stimulus becomes catastrophic as p approaches 1, i.e. the regularised $E(p)$ will go to zero. This catastrophic effect of damage accumulation as p approaches 1 is a reasonable improvement over the original inception in HMRR, which remains bounded as p approaches 1. In Section 3, we will prove this fact. However, we argue that a catastrophic damage accumulation term, meaning that the damage will become irreparable and grow toward $D = 1$, is phenomenologically associated with fatigue rather than the value of the porosity. This motivates our looking in Section 4 at an alternative damage accumulation model.

Table 1. Model constants and other parameters defined, given or derived.

Symbol	Value	Units	Definition
c_1	–	1	$\mathrm{e}^{-k_b k_c}$
c_2	–	days^{-1}	k_b
c_3	–	1	$\frac{f_{a(\max)} - f_{a0}}{f_{a0}} \mathrm{e}^{-k_r f_{a(\max)}}$
c_4	–	mm	$\frac{k_r}{D_0} f_{a(\max)}$
c_5	–	mm/mm^2	
c_p	1.90		See Equation (18)
K_D	5.57×10^4	mm/mm^2	
A_0	2.84×10^{-2}	mm^2	–
$f_{a(\max)}$	0.5	mm^{-2}/days	–
m	–	1	See Equation (18)
T_R	24	days	–
T_I	8	days	–
T_F	64	days	–
R_L	3000	days^{-1}	–
k_b	6.5×10^{10}	days^{-1}	–
k_c	9.4×10^{-11}	days	–
k_r	-1.6	mm^2 days	–
p_0	–	1	See Equation (13)
D_0	0.0366	mm/mm^2	–
Φ_0	1.875×10^{-10}	days^{-1}	–
f_{a0}	0.0067	# BMU's/mm^2/day	–
F_s	5	mm^{-2}	See Equation (14)

The mechanical stimulus is very sensitive to changes in $E(p)$ and $S(p)$ via p in the following sense: the relative sensitivity $|(\partial\Phi/\partial E)/\Phi|$ for the range of values of E given in Figure 1(a) is small (less than 10^{-3}, in fact). On the other hand the relative sensitivity of Φ to p, when E and S are fitted with high order polynomials, is large. Using a significantly lower order fit for E and S will reduce the sensitivity of the mechanical stimulus to changes in p to reasonable levels. The empirical functions $E(p)$ and $S(p)$ in Figure 1(a),(b) are not very intricate, suggesting that a lower order polynomial fit would be suitable. We fit the data with second degree polynomial expressions for both Equations (9) and (10), and found that the results changed very minimally compared to using the higher degree polynomial counterparts, especially with regard to final steady states. Piece-wise cubic splines do an even better job at following the higher order polynomial fit for $S(p)$ and $E(p)$ for the full range of p with a marginal increase in numerical sensitivity. We conclude that a spline, quadratic or cubic polynomial interpolant would be a simpler, and possibly more accurate, approach to interpolate the data.

2.3 Model parameters

In our analysis, we use the HMRR parameter values shown in Table 1. The table indicates if the parameters are derived, given (e.g. experimental/observational in origin), or defined based on constraints. Note the large variation in the size of the parameters in the table. This variation requires that special attention be given to the numerical implementation of the model to prevent serious loss-of-precision errors, even on double precision machines, and further, that we are careful to take into account the origin of the parameters, so as to avoid inconsistent model results.

The mechanical stimulus Φ_0 is a given parameter. Its value is what is required to maintain cortical bone mass in equilibrium and corresponds to an average person who experiences about $R_L = 3000$ cpd of lower extremity loading. The cyclic strain is taken as 500 $\mu\varepsilon$ (equivalent to a compressive force of 891.6 N). The initial damage $D(t=0) = D_0 = 0.0366\,\text{mm/mm}^2$ is the average crack density for a 40-year-old man. In HMRR, this value was obtained from measurements. The parameter $f_{a0} = 0.0067$ # BMU's/mm^2/day is given. The initial porosity, $p(t=0) = p_0$, is a derived parameter, dependent on q, and is defined by solving for the root p_0 of the equation:

$$\Phi(p_0) = \Phi_0 = 3000\left(\frac{891.6}{100E(p_0)}\right)^q. \tag{13}$$

(Note, that the calculations in the HMRR paper used the same p_0 for all values of q, see Figure 7 of Hazelwood et al. 2001.)

The given value of the mechanical stimulus $\Phi_0 = 1.875 \times 10^{-10}\,\text{days}^{-1}$ maintains a cortical bone mass in equilibrium, and is consistent with a value of 891.6 N for the load, and $q = 4$, $p = p_0$ in Equation (13). Thus at equilibrium $\dot{D} = 0$ in Equation (2) and we define the damage rate coefficient K_D as

$$K_D = \frac{F_s D_0 S(p_0) f_{a0} A}{\Phi_0} \approx 5.57 \times 10^4\,\text{mm/mm}^2. \tag{14}$$

The factor $S(p_0)$ is needed to normalise the damage rate coefficient appropriately at $t = 0$ in Equation (2). In the HMRR calculations in Hazelwood et al. (2001), the authors did not include the factor $S(p_0)$ and its damage rate coefficient is $K_D/S(p_0) \approx 1.85 \times 10^5\,\text{mm/mm}^2$. We use K_D unless otherwise noted. The initial bone activation frequency f_{a0} was taken to be 0.00670 exactly, we do so here as well. However, when calculating f_a they also take into account the greater potential for remodelling offered by large surface areas, i.e. $S(p)$, but neglect to include this in the calculation of K_D (see Equation (9) of Hazelwood et al. 2001). The constant $q = 4$ is chosen to maintain balance between bone formation and removal (cf. Martin, 1995; Martin et al. 1998).

3. Analysis of the MBM

The steady states of the model are found by setting the time derivatives of p and D to zero in the evolution equations (1) and (2). In what follows we analyse the model as originally conceived by the authors of HMRR. However, we used the corrected value of K_D. We define the asymptotic steady state solutions by $p(t) \to \hat{p}$ and $D(t) \to \hat{D}$ as $t \to \infty$. The physically relevant steady state solutions satisfy $\hat{D} \geq 0$ and $0 \leq \hat{p} \leq 1$, are stable, and describe the asymptotic behaviour of the model. At steady state, the Equations (1) and (2) reduce to:

$$Q_R N_R(\hat{p}, \hat{D}, t) = Q_F N_F(\hat{p}, \hat{D}, t), \tag{15}$$

$$K_D \Phi(\hat{p}, \hat{D}) - F_s A \hat{D} f_a(\hat{p}, \hat{D}) = 0, \tag{16}$$

where $\Phi(\hat{p}, \hat{D}, t) = \hat{\Phi}$, $A(\hat{p}) = \hat{A}$, $E(p) = \hat{E}$ are all constant.

Figure 2 plots the steady solution with a load $L = 891.6$ N. The figure compares the outcomes of using the corrected damage rate coefficient K_D with the solutions derived with $K_D/S(p_0)$, the value used throughout by the authors of HMRR. The differences in the damage are significant over the entire range of porosity. Figure 3 shows the steady-state solution curves in an under-stressed ($L = 255$) and an over-stressed ($L = 1665$) situation. In the under-stressed case, there is very little damage when the porosity is small. Then, as $p \to 1$ the damage in the steady state solution increases rapidly until about $p = 0.95$ when it quickly drops. The sudden drop in the damage, for large p, is caused by the downstream effects of Φ, which in turn is being affected by the increasing value of E. (In this instance we are using the original expression of $E(p)$ as in Equation (8).) More specifically the damage repair term is capable of arresting the damage because while p is large it does not necessarily lead to a large damage

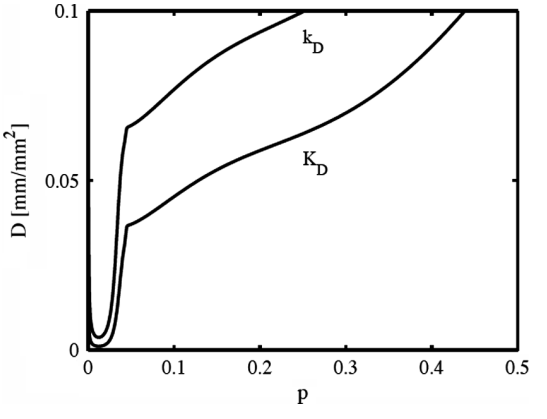

Figure 2. The damage in the steady state solution is plotted in the (p, D) plane for the load $L = 891.6$ N for both the correct damage rate coefficient f and for $K_D/S(p_0)$. The model predicts vastly different damage to the steady state solution for the two cases.

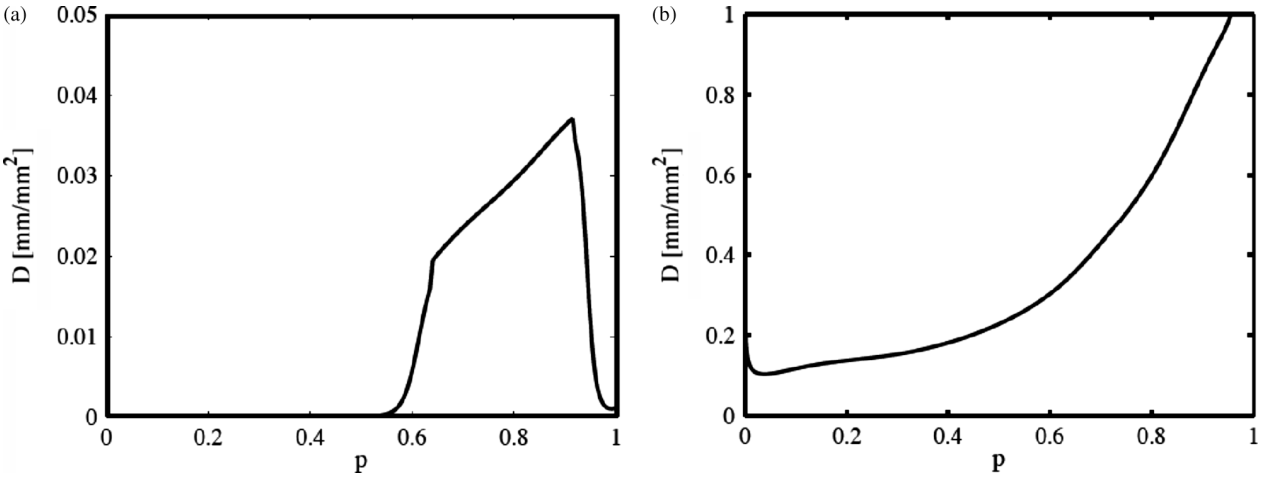

Figure 3. The fixed point curves for K_D under-stressed: (a) $L = 255$, and over-stressed: (b) $L = 1665$. The plot in the (p, D) plane shows that in the under-stressed low porosity case, the damage is insensitive to the porosity when $p < 0.5$.

accumulation term since $E(p)$ is finite and non-monotonic for large p.

In other words, the behaviour of the model is suspect for large p and mild loads. In the over-stressed case, there is a sensible and dynamic interplay between porosity and damage for small p. The damage in the steady state solution continues to increase as p gets larger until D reaches very large but finite values at large p. For $p > 0$ we have $f_a(D, p) > 0$, since $S(p)$ and $\Phi(p)$ are bounded and positive and $E(p) > 0$.

From Equation (2), we know

$$\frac{\mathrm{d}D}{\mathrm{d}t} \leq g_1 - g_2 D,$$

where g_1, g_2 are positive and do not depend on D. This implies $D(t) \leq C_1(g_1, g_2)$, where C_1 is a positive constant that depends on the parameters in g_1, g_2. Hence, the model does not produce solutions with super linear growth, as those observed numerically in Hazelwood et al. (2001) for the HMRR model.

Since the model produces steady bounded solutions, one might wonder if it is capable of producing non-steady state asymptotic solutions, e.g. oscillations. Decaying oscillations in the porosity and activation frequency were observed for the first few hundred days in Figures 5 and 8 of Hazelwood et al. (2001). To investigate the possibility of asymptotic oscillating solutions, we perturb the HMRR steady solutions $(p(t), D(t)) = (\hat{p}, \hat{D}) + (\delta p, \delta D)$ and substitute them into Equations (1) and (2). We obtain $\mathrm{d}\delta p/\mathrm{d}t = 0$ and the damage equation leads to

$$\frac{\mathrm{d}\delta D}{\mathrm{d}t} = -\kappa_1 \delta p - \kappa_2 \delta D,$$

where the real part of $\kappa_i \geq 0$, $i = 1, 2$, and are never strictly imaginary. Therefore, if oscillations appear, they decay exponentially; sustained oscillations are not possible. The analysis does not support the resurgence of high frequency oscillations that spontaneously appear after about 400 days (as in Figure 4 of Hazelwood et al. 2001). We are unable to reproduce this effect in our stabilised model and speculate that these higher frequency oscillations be numerically induced. (See Section 5 for further details on this issue).

4. Improving the damage rate model

Experiments, e.g. those reported by Caler and Carter (1989), Pattin et al. (1996) and Cotton et al. (2003), have

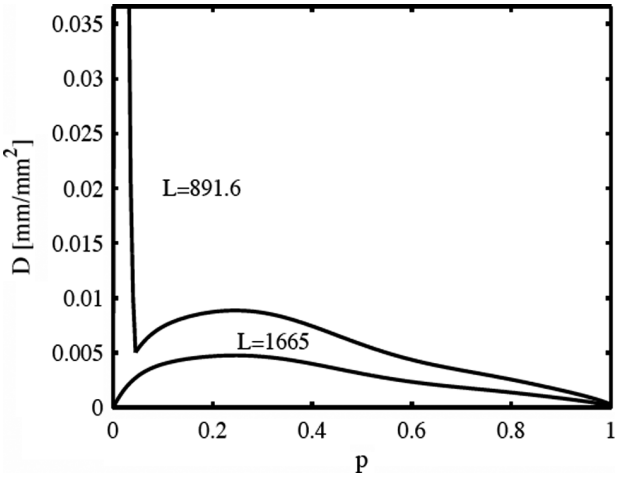

Figure 4. Porosity and damage steady state curves, using (18) with $m = 1$ for the damage equation. The value of c_m was tuned for the under-stressed $L = 891.6\,\mathrm{N}$ load where steady solutions exist for $p > p_0 = 0.0442$, even though the damage is catastrophic for $p < p_0$. Steady solutions exist for loads higher than $L = 891.6\,\mathrm{N}$ for all values of p and D. Notice the reduced damage for high porosity in the over-stressed case, $L = 1665\,\mathrm{N}$.

amply demonstrated that under over-stressed conditions, the damages would accumulate and eventually the bone would fail. The damage in the HMRR, as we demonstrated in the previous section, is bounded for all loads. To improve the model at high stress levels, we replace the damage growth term with a physically based Paris-like fatigue model, as used in similar fatigue damage models (Taylor and Prendergast 1997).

Pattin et al. (1996) (also Caler and Carter 1989) perform an empirical fit of the creep strain of cortical bone subjected to strains. The bone specimens come from cadavers and are thus not subject to damage repair. The data show that when the cyclic strain in the bone exceeds some threshold then there is progressive damage to the bone. This damage can eventually grow to catastrophic levels, provided the load is sufficiently high and/or the sample is subjected to stresses for long enough periods of time. Furthermore, the data show that the history of bone degradation depends on whether the stresses are compressive or tensile.

To extend the model for catastrophic damage, we use a Paris-like damage law of fracture mechanics for the permanent strain (Suresh 1991), that relates the crack growth rate under a fatigue stress regime to the stress intensity factor as a power law. Hence, for $D > D_{\text{th}}$, threshold damage is

$$D = \frac{1}{F[(t_f - t)^{\alpha}]}, \tag{17}$$

in terms of some function F to be determined. Below that threshold $D = D_{\text{th}}$, D is constant. For the sake of discussion, this form ignores damage repair. We adopt the damage repair term of the original HMRR in the improved damage rate equation. Here, t_f depends on L and E, as suggested by (7). We will show that Equation (17) would be qualitatively similar to the data presented in Cotton et al. (2003) in their Figure 3, i.e. a period of accumulating damage followed by catastrophic failure, given repeated loading above some threshold, and can be made to fit the data studied by Pattin et al. (1996). We thus offer an alternative and perhaps simpler description of the damage accumulation term.

To better account for bone failure, we investigated replacing the logarithmic fit suggested in Pattin et al. (1996) with a power-law dependence for the relative damage $\bar{D} \equiv D/D_{\text{th}}$:

$$\frac{\mathrm{d}\bar{D}}{\mathrm{d}t} = c_m \left(\frac{L}{E(p)}\right)^q \bar{D}^m \bar{D} - F_s A \bar{D} f_a(p, \bar{D}), \tag{18}$$

for $D \geq D_{\text{th}}$, where $c_m \geq 0$, and $m \geq 1$. If $D < D_{\text{th}}$, then D is constant. In the under-stressed case, replacing the logarithmic damage growth term in Equation (2) with the power-law model makes almost no difference. However, when the bone is severely over-stressed, then the power-law model significantly increases the bone damage.

We follow the HMRR approach in defining an equilibrium damage state where c_m is tuned to obtain $\mathrm{d}\bar{D}/\mathrm{d}t = 0$ for a specific load, e.g. $L = 891.6\,\text{N}$, $E(p_0)$, f_{a0} and $D = D_0$. The exponent m is a new parameter, whose numerical value in the example calculations will be taken to be 1; the reason for this choice of m will become apparent in what follows.

A threshold for the relative damage to grow exponentially and irretrievably is given by

$$\bar{D} > \left(\frac{F_s A f_a E^q}{c_m L^q}\right)^{1/m},$$

when the damage accumulation is more prominent than the damage repair term. Note that increasing the load L lowers the threshold and that the larger the load, or the exponent m, the sooner the instability occurs. Blowup leads to full decoupling of the activation frequency on the damage, i.e. $f_{a(\text{damage})} = f_{a(\max)}$, and no feedback is possible in the porosity, other than a readjustment in the porosity. Thus, the coupled model exhibits continuous growth in the damage with no change on the porosity, beyond an adjustment in its value shortly after the blowup. Whether this is the correct behaviour of under-stressed bone is beyond the scope of this work. Figure 4 shows the critical points in the (p, D) plane for $m = 1$. The case corresponding to $L = 891.6\,\text{N}$ is a tuned threshold for the model (the c_m is set with this load). Interestingly, steady solutions exist for porosities higher than about 0.0442, which is the value of p_0. For loads higher than $L = 891.6$, steady solutions are defined for all values of p and D. These higher load cases generate curves that would be located below the $L = 891.6$ curve. The quick decrease in the damage for high porosity in the over-stressed case (where we take $L = 1665$), is related to the anomalous increase in E for high values of p (see Figure 1(a)).

The evolution of the porosity, damage and activation frequency for the new model are shown Figure 5(a) for the over-stressed case. As expected in over-stressed conditions, provided enough time passes, the damage can grow exceedingly large, leading to bone failure. The model can also have catastrophic damage in the middle to high range of $0.3 < p < 0.8$ if the bone is stressed repeatedly. This can also happen if the material is very sensitive to damage because its Young's modulus is low. The most salient feature of the solution is the exponential growth. In the under-stressed case, we get solutions that are qualitatively and quantitatively similar to those obtained by HMRR: compare Figure 5(b) and (c). In the under-stressed cases, the damage repair term dominates in the new model, this is not the case for the original HMRR model solution.

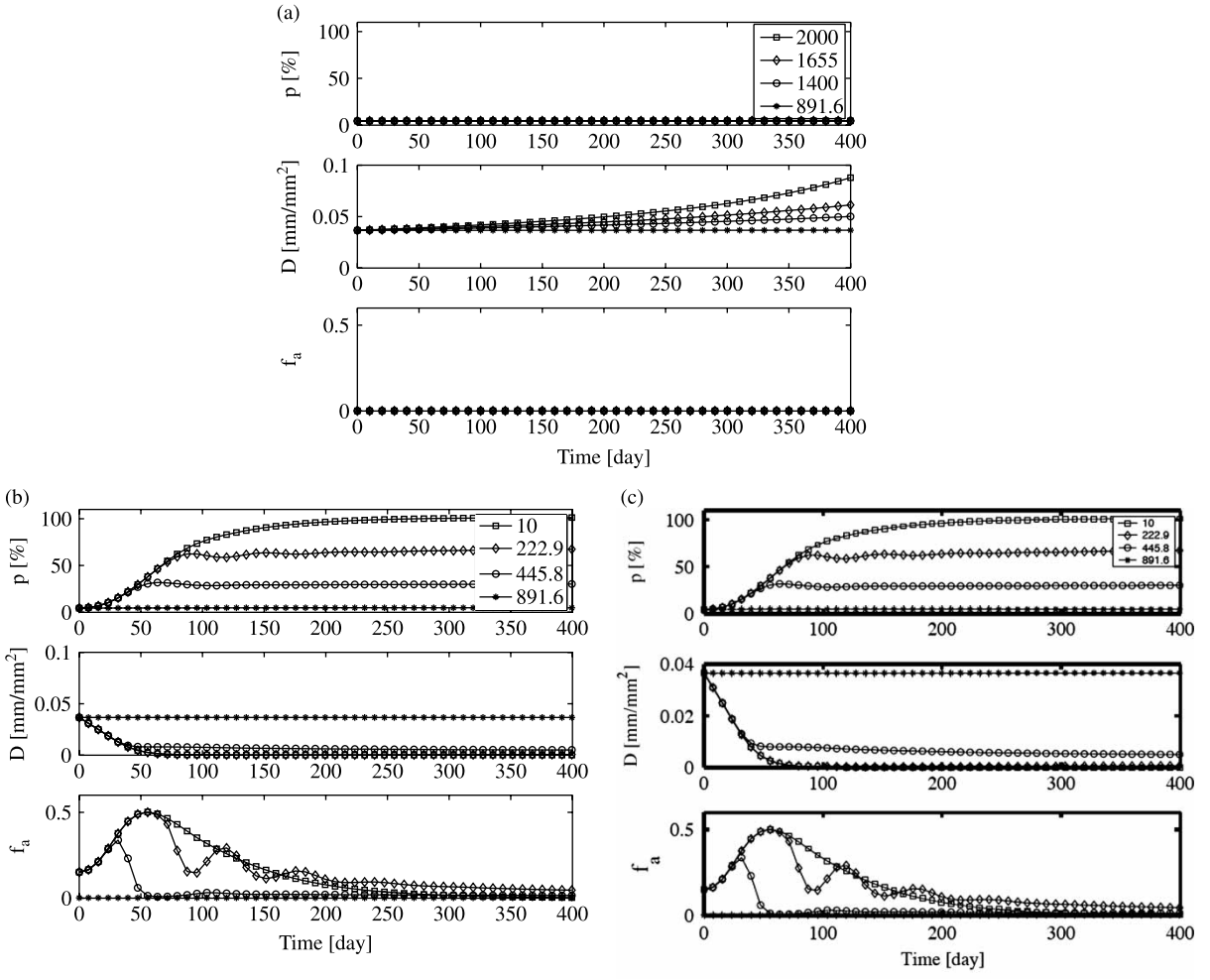

Figure 5. Porosity, damage and activation frequency as a function of time, using (18) with $m = 1$. (a) Over-stressed for the loads $L = 891.6$, 1400, 1655 and 2000 N. Notice how in the over-stressed case the damage continues to grow exponentially, which will eventually lead to bone failure. The HMRR, over-stressed case will have growth, but it will be linear in time. (b) Under-stressed for the loads $L = 10$, 222.9, 445.8 and 891.6 N. (c) The solutions for under-stressed case are plotted for the loads $L = 10$, 222.9, 445.8 and 891.6 N, and corresponding to solutions in Figure 4 of HMRR. The oscillations are less pronounced than the HMRR solutions. We did not observe the bursting behaviour of the HMRR solutions, and speculate that they are numerical artefacts.

5. Comparison with other models

García-Aznar et al. (2005) defined the damage as $\mathcal{D} := 1 - E/E_0$, where E_0 corresponds to a reference value of the elastic modulus of the undamaged bone. They adopted a form for the damage accumulation term, consistent with the logarithmic fit suggested in Pattin et al. (1996),

$$\mathcal{D} \propto b_1 - b_2[\ln(b_3 - c_g t/t_f)]^n, \tag{19}$$

where b_1, b_2 and c_f are constants tuned to agree with results in Pattin et al. (1996). Moreover, they defined two different damage formation modes, one for tension and one for compression. The rate in both cases is essentially exponential in the damage itself. Under tensile stress, they used $n = 1/2$, $b_1 = 1$, $b_2 > 0$, $0 < b_3 < 1$; under compression, they used $n = 1$, $b_1 = 0$, $b_2 > 0$, $b_3 = 1$.

We use the same definition of the damage, but define the damage equation by the power law: for $\bar{D}$, ignoring damage repair, and with $\mathcal{D} = \bar{D} - \mathcal{D}_0$, is of the form

$$\mathcal{D} \propto \frac{b_4}{(1 - c_f t/t_f)^{1/m}} - \mathcal{D}_0, \tag{20}$$

where b_4 can be written in terms of m, t_f and c_f.

Both forms can be made to pass through $\mathcal{D} = 0$ at $t = 0$ with proper tuning of the parameters. Both exhibit divergent behaviour, at $t_f b_3/c_g$ and t_f/c_f, respectively. The values of the parameters in the exponential damage accumulation term appear in García-Aznar et al. (2005), in both the compressive and the tensile cases. They are

chosen to match the fit suggested by Pattin et al. (1996). Assuming that Equation (19) is exact in its representation of the damage accumulation due to stresses one can write a series about $t = 0$ of Equations (19) and (20). Term by term comparison shows that for both tensile and compressive forces $m = 1$, and that $\mathcal{D}_0 = b_4$ is the compressive case and $\mathcal{D}_0 \neq b_4$ for the tensile case. Both of these parameters can be fixed uniquely for a reasonable fit. This implies that both the exponential and the power law fits are equally capable of fitting the experimental data, i.e. they are both qualitatively similar and since the logarithmic fit is benchmarked against data, the power-law formulation can be made to fit the data as well. (Of some mathematical interest, writing a series expansion near the singular point, a Laurent expansion for the powers of the logarithm function shows that the leading order behaviour requires a complex representation. This is obviously not the case for the power law representation.)

We now turn to considering how the above model would relate to a non-biologically-based bone remodelling model that takes into account micro and macrocracks. The model advocated by Taylor and Prendergast (1997), paraphrased is

$$\frac{\mathrm{d}\bar{D}}{\mathrm{d}t} = \left(\frac{L}{E(p)}\right)^q \Big[c_M(\bar{D} - \bar{D}_{\mathrm{th}})^m(\bar{D} - \bar{D}_{\mathrm{th}})\mathcal{H}(\bar{D} - \bar{D}_{\mathrm{th}}) + c_\mu \bar{D}^m \bar{D}(1 - \bar{D})^{m'}\big(\mathcal{H}(\bar{D}) - \mathcal{H}(1 - \bar{D})\big)\Big]. \tag{21}$$

Here $\mathcal{H}(\cdot)$ is the Heaviside function. We define $D_{\mathrm{tr}} = D_0$, where D_0 is the microstructural barrier (typically in the order of 100 μm) and $\bar{D} = D/D_{\mathrm{tr}} = D/D_0$. In Taylor and Prendergast (1997), $m = 1.75$ and $m' = 5$. The constants c_M and c_μ and q are experimentally derived fitting constants. The first term on the right hand side accounts for the damage accumulation term in Equation (18). The second term is a damage accumulation term that is associated with microcracks. Figure 6 illustrates the typical behaviour of $\mathrm{d}\bar{D}/\mathrm{d}t$ for small (dashed line) and large (solid line) loads.

Note that for a specific load and below, there is a range in $\bar{D}$ over which $\mathrm{d}\bar{D}/\mathrm{d}t \approx 0$ when all the other parameters are fixed. We call this the no-growth gap. Below this gap there is microcrack damage; above this gap there is macrocrack damage, because outside of this gap $\mathrm{d}\bar{D}/\mathrm{d}t > 0$. The implication is that if $\bar{D}(t = 0)$ is in the microcrack range, it will grow to some size and then stop, if the gap is of bigger than or equal to 1 value of $\bar{D}$. However, if $\bar{D}(t = 0)$ is above the gap values (or there is no gap), there will be catastrophic damage to the bone.

The Taylor and Prendergast model equation (21) requires $\bar{D}_{\mathrm{th}}$ be a load-dependent parameter and explicitly models the microcracks. On the other had, in the HMRR $\bar{D}_{\mathrm{th}}$ is interpreted as the threshold between microcrack and

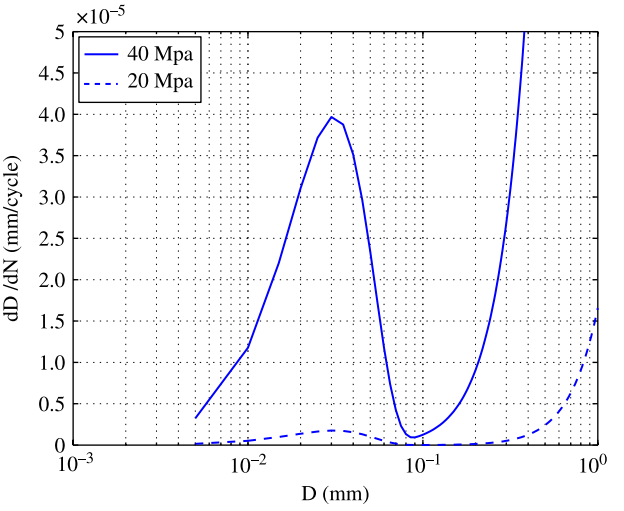

Figure 6. Damage rate, for stresses for small 20 MPa (dashed) and large 40 MPa (solid line) loads, as proposed by Taylor and Prendergast (See Figure 3 in Taylor and Prendergast 1997.) The derivative $\mathrm{d}\bar{D}/\mathrm{d}t \approx 0$ N ear $\bar{D} = 10^{-3}$ creates a no-growth gap in the damage. Below this gap there is microcrack damage; above this gap there is macrocrack damage.

macrocrack damage. Taylor and Prendergast's model does not have a biologically based repair term, hence macrocracks will never disappear, but increase irretrievably under persistent cyclic load. The HMRR model allows for the possibility that biologically based repair occur. Although the Taylor and Prendergast's model can replace the damage accumulation term in HMRR, it does not have a biologically based repair term. The importance of this term for modelling live bone still needs experimental verification.

Our model is a recasting and extension of the MBM first proposed by HMRR (Hazelwood et al. 2001). In our reformulated model, we used the value of the proportionality constant in Equation (2), which includes the factor of $S(p_0)$, i.e. K_D. Figure 5(b),(c) shows qualitative agreement of our model with the original HMRR for under-stressed cases. Our solutions do not exhibit any of the spurious numerical artefacts in the original HMRR such as the oscillations observed in Hazelwood et al. (2001). Also, in contrary to the HMRR model, the converged solutions remain bounded in the over-stressed cases. However, this restriction is removed in the alternative model proposed here. See damage plot in Figure 5(a).

Of special consideration is the activation frequency in Figure 5(c) for the case of $L = 445.8$ N, which contrasts with HMRR in Figure 4, where the latter appears to oscillate significantly. As we mentioned in the Section 3, it is not possible to obtain sustained oscillations in the dynamic variables p and D. Oscillations, however, are not ruled out, and in fact often occur in delay equations. The oscillations that appeared in the HMRR result for dynamic variables

in the transient period, however, are mostly a numerical artefact. Longer-period oscillations in the HMRR results related with the dynamic variables, *not* associated with changing the parameters T_I, T_R and T_F, were most likely induced by allowing p and D to go out of range (inducing complex eigenvalues in the linearised equation). The oscillations in the activation frequency observed in the original HMRR results were ascribed to changes in $f_{a(\max)}$. These oscillations, shown in Figure 5(c) for $L = 222.9$ N, are more pronounced in the original HMRR than in our regularised model. We found as the load increases from 240 to 400 N the decaying oscillations in f_a increase. These oscillations disappear well outside of this load range. Although the parameters T_R, T_I and T_F are set by nature, changes in these parameters can also create decaying oscillations. The frequency and decay of the oscillations can be determined by analysing the spectrum of the linear operator associated with the delay equations and have been verified in numerical simulations.

Overloading, as shown in Figure 6 of HMRR for $L = 1655$ N, leads to exponentially growing porosity and activation frequency. Figure 7 of HMRR shows that $q = 8$ leads to similar exponential growth in porosity and damage. These simulations are in agreement with our boundedness estimates for small porosities when the damage is bounded. When p approaches 1, then the simulations using the original HMRR polynomial approximation of the Young's modulus still do not predict bone failure when the model is over-stressed, and the solution does not exhibit super-linear growth, in agreement with our estimates in Section 3. We observed that increasing $f_{a(\max)}$ decreases the damage and has less effect for smaller p and D. Varying $f_{a(\max)}$ moves the steady-state solutions of the solution as shown in Figure 7.

6. Discussion

Bone remodelling is a complex process involving dynamics of multiple scales from signalling to cell activities and organ level mechanics. The model proposed by Hazelwood et al. (2001) started an important advancement in modelling of bone remodelling, byintegrating the cellular activities of BMUs with the macroscopic stress strain mechanics of the bone. We recast and analysed an extended MBM of HMRR (Hazelwood et al. 2001). The recast model simplified the structure and made the equations more amenable to mathematical analysis. The modified model is well balanced and more numerically stable, even with the extreme spatio-temporal parameter scales. This eliminated some serious numerical loss-of-precision errors that could dominate the behaviour of the original model. The analysis of the steady states of the model was used to unravel the global behaviour of the solutions for a fixed load L. For a fixed set of bone parameters, dynamic behaviour can be fully characterised by the load. Furthermore, knowing the global solutions it was also possible to suggest phenomenological simplifications of the model that lead to the same qualitative behaviour.

Even with the regularised formulation for the Young's modulus, we found that the dynamics of the 'mechanical stimulus' Φ limited, and this leads to problems in the HMRR damage equation. Furthermore, all solutions of the equation with the HMRR formulation for the damage equation are bounded, regardless of the level of the stress on the bone. We formulated a revised power-law damage-causing term that does not depend on the mechanical stimulus motivated by the bone data analysed in Cotton et al. (2003) that show creep strain behaviour

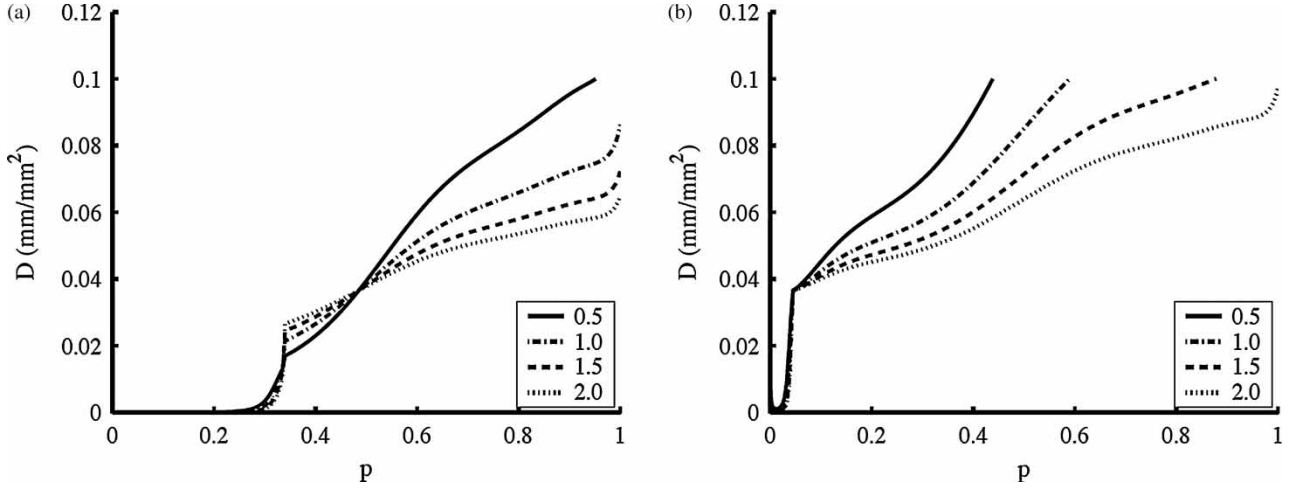

Figure 7. The effect of increasing $f_{a(\max)}$ from 0.5, 1.0, 1.5, to 2.0 on the steady-state solutions for the damage as a function of porosity. (a) $L = 445$ N, (b) $L = 891.6$ N. Note how the damage is significantly reduced as $f_{a(\max)}$ increases, except in a small region of the $L = 445$ N case. We observed that increasing $f_{a(\max)}$ has less effect when p and D are small.

and possible failure under loading. The power-law damage equation was able to capture a wider range of dynamical behaviour.

The new damage rate equation has a Paris-like damage accumulation term and a BMU activity-dependent repair term when the damage is above a threshold value D_{th}. The damage is constant if it is below some threshold value. The purely mechanical remodelling damage equation of Taylor and Prendergast (1997) provides a mechanistic and load dependent for the threshold D_{th} over which $\mathrm{d}\bar{D}/\mathrm{d}t > 0$, interpreting D_{th} in (18) as the load-dependent threshold between microcracks that are responsible for a screening effect in the stresses, and macrocracks that are capable of weakening the bone. While we find that their complex modelling description of the screening is potentially relevant to bone tissue dynamics, the model does not take into account any biological repair mechanisms, such as the damage repair term suggested in HMRR. The importance of this term in bone remodelling still needs to be accessed experimentally by comparing fatigue damage of live and dead bones under a variety of loading conditions. If the BMU activity-based repair term is important then it should be possible to measure that $\mathrm{d}\bar{D}/\mathrm{d}t$ can actually decrease, in the macrocrack range, in the live bone. With our new damage rate equation, we showed that the resulting model agrees qualitatively with the original HMRR model in the under-stressed case, and for the over-stressed case, is capable of catastrophic damage if the constant load is large enough. We have suggested how the stress screening and the damage repair can coexist.

Our calculations of the original HMRR model indicated that the dependence of the porosity on the damage might be too weak, particularly in the over-stressed case, where it is possible to get unrealistic values in the damage with little change in the porosity. Because the coupling between porosity and damage is weak, the stability of the system is controlled by the damage equation and is almost independent of the porosity, and the critical point for the solution is unstable. We found that making the damage rate relative to the damage itself leads to significant improvements for the over-stressed case.

Our analysis of the dynamical behaviour of the solutions demonstrated that the material properties and parts of the activation frequency function could be approximated by a simpler constitutive equation, without loss of quantitative and qualitative fidelity. The fact that this can be done points to the possible room for model improvement. The HMRR MBM model specifies the material properties of the bone, i.e. the effective surface area and the Young's modulus, are entirely fitted to data in terms of porosity. This leads to weak coupling in the steady solutions of the porosity and the damage under fixed loads. In contrast, the material properties are in terms of both the porosity and the damage in the García-Aznar et al. MBM model. In García-Aznar et al. (2005), the authors opted for a different model for the Young's modulus by taking into account the loss of stiffness due to damage and with this change they obtained a richer phenomenology. It strongly suggests that the improvements in the HMRR formulation of the MBM model could be obtained by focusing on more realistic models for the material properties of the bone.

The recent phenomenological model of García-Aznar et al. (2005) is capable of modelling stress fractures and has been shown to have significant predictive potential. Beneath the phenomenological complexities, this model shares many characteristics with the MBM. They both use a population dynamics equation for the BMU's and an equation for the damage rate that involves a formation and a repair term. Our Paris-like damage production law is very close to the García-Aznar et al exponential damage production term. We have shown that our modification of the HMRR model makes it qualitatively consistent with experiments and also similar to other MBM models. Both of these damage accumulation terms give qualitatively similar fits of the damage data from experiments.

In summary, for the highly non-linear equations for bone remodelling models, the computed solutions are sensitive to numerical errors, which can introduce artefacts into the simulations. We reformulated the model to minimise these errors and demonstrated that the numerical solution was better conditioned and consistent with the theoretical estimates on steady solutions. We derived and analysed the stationary solutions of the model, for all values of damage and porosity. These stationary solutions capture the asymptotic behaviour of the model and can help guide extending the model to better account for the biologically based features in bone remodelling. The extended model retains qualitative consistency with the HMRR model in the under-stressed case, but allows for the possibility of irreparable failure under the right loading and when the damage repair term is unable to arrest the damage accumulation. We showed that the extended model is similar with regard to damage accumulation and BMU activity to an MBM model by García-Aznar et al. (2005).

Acknowledgements

The authors are grateful to Scott Hazelwood and Chris Jacobs for several comments and suggestions. This work was performed in part while JMR was a PIMS faculty visitor at Simon Fraser University and a visitor at Los Alamos National Laboratory. JMR was supported by NSF Grant DMS-327617 and DOE Grant DE-FG02-02ER25533. RC was supported by an NSERC Canada Discovery Grant. YJ and JMH were supported by the US Department of Energy under Contract No. DE-AC52-06NA25396.

References

Caler W, Carter DR. 1989. Bone creep fatigue damage accumulation. J Biomech. 22:625–635.

Cotton JR, Zioupos P, Winwood K, Taylor M. 2003. Analysis of creep strain during tensile fatigue of cortical bone. J Biomech. 36:943–949.

Doblaré M, García J, Gomez M. 2004. Modelling bone tissue fracture and healing: a review. Eng Fract Mech. 71:1809–1840.

García-Aznar JM, Rueberg T, Doblaré M. 2005. A bone remodelling model coupling microdamage growth and repairing by 3D BMU-activity. Biomech Model Mechanobiol. 4:147–167.

Hazelwood SJ, Martin RB, Rashid MM, Rodrigo JJ. 2001. A mechanistic model for internal bone remodeling exhibits different dynamic responses in disuse and overload. J Biomech. 34:299–308.

Hernandez CJ, Beaupré GS, Carter DR. 2000. A Model of mechanobiologic and metabolic influences on bone adaptation. J Rehabil Res Develop. 37:235–244.

Hernandez CJ, Beaupré GS, Keller TS, Carter DR. 2001. The influence of bone volume fraction and ash fraction on bone strength and modulus. Bone. 29:74–78.

Iserles A. 1996. A first course in numerical analysis of differential equations. Cambridge: Cambridge University Press.

Martin RB. 1992. A theory of fatigue damage and repair in cortical bone. J Orthop Res. 10:818–825.

Martin RB. 1995. Mathematical model for repair of fatigue damage and stress fracture in osteonal bone. J Orthop Res. 13:309–316.

Martin RB, Sharkey NA, Burr DB. 1998. Skeletal tissue mechanics. New York: Springer Verlag.

Nyman JS, Yeh OC, Hazelwood SJ, Martin RB. 2004a. A theoretical analysis of long-term biphosphonate effects on trabecular bone volume and microdamage. Bone. 35: 296–305.

Nyman JS, Hazelwood SJ, Rodrigo JJ, Martin RB, Yeh OC. 2004b. Long stemmed total knee arthroplasty with interlocking screws: a computational bone adaption study. J Orthop Res. 22:51–57.

Pattin CA, Caler WE, Carter DR. 1996. Cyclic mechanical property degradation during fatigue loading of cortical bone. J Biomech. 29:69–79.

Suresh S. 1991. Fatigue of materials. Cambridge, UK: Cambridge University Press.

Taylor D, Prendergast PJ. 1997. A model for fatigue crack propagation and remodelling in compact bone. Proc Inst Mech Eng. 211:369–374.

Wang X, Ni Q. 2003. Determination of cortical bone porosity and pore size distribution using a low field pulsed NMR approach. J Orthop Res. 21:312–319.